The Development of a Closed-Form Expression for the Input Impedance of Power-Return Plane Structures

Minjia Xu, *Member, IEEE,* and Todd H. Hubing, *Senior Member, IEEE*

***Abstract*—In multilayer printed circuit boards, the noise on the power bus is influenced by the impedance between the power and ground planes. Power-bus noise estimates require an accurate estimate of the power-bus input impedance. This paper develops a closed-form estimate of the input impedance for circular power-return plane structures. When the structure is lossy (e.g., boards employing embedded capacitance or densely populated boards), the energy reflected from the board edge does not significantly affect the input impedance. In general, the expressions developed here for circular structures can be used to estimate the impedance of lossy power-return plane structures of any shape.**

***Index Terms*—Power-bus impedance, power-bus modeling, power-bus noise, power plane, radial transmission line, return plane.**

I. Introduction

POWER-BUS noise suppression can be a critical issue in high-speed printed-circuit-board (PCB) and multichip-module (MCM) designs. Common sources of power-bus noise include sudden surges of current drawn by digital devices as they switch states. If the transient noise voltage exceeds the noise margin of another active device connected to the power bus, the design may not work properly. Consequently, it is important to be able to estimate the maximum power-bus noise early in a board's design cycle to ensure the signal integrity and electromagnetic compatibility of the product.

In order to supply the large amount of current demanded by active devices while avoiding significant changes in the power-bus voltage, power distribution networks in PCBs and MCMs are generally designed to have very low impedance over a broad range of frequencies. The impedance associated with active devices mounted on the board surface tends to be much higher than the power-bus impedance. Therefore, most active devices can be modeled as current sources [1]. The power-bus noise voltage at one location due to the current drawn by a component at another location can be calculated using the equation

$$V_{\text{noise}} = I_{\text{device}} \times Z_{21} \tag{1}$$

where Z_{21} is the power-bus transfer impedance between these two locations. Several texts and papers have proposed methods to estimate the total transient current drawn by active devices (e.g., [1]–[3]). Once the total noise current is determined, the magnitude of the power-bus noise voltage can be determined at any given frequency from an estimate of the power-bus transfer impedance between the source and the observation locations.

Current multilayer PCBs and MCMs often use solid power-return plane pairs for power distribution. With the interaction of vias and devices connected to the power bus (for example, active components, connectors, decoupling capacitors, etc.), it is very difficult to quantify the exact behavior of the entire power distribution system. Though general, full-wave modeling methods such as finite difference time domain (FDTD), finite element method (FEM), method of moments (MoM), and partial element equivalent circuit (PEEC) have been applied to model PCBs and MCMs with power-return plane pairs successfully, these models are relatively complex. In addition, they require a significant amount of time and expertise to implement properly.

In addition to full-wave models, several investigators have used a cavity model to characterize the rectangular power-return plane pair fed by a current source (e.g., [4] and [5]). By modeling an unpopulated power-return plane pair as a TM_z cavity, the input and the transfer impedance can be expressed as double-infinite sums. Recently the double-infinite series expression was further reduced to a single-infinite series by applying a summation formula of a Fourier series [6]. Although the power-bus input and transfer impedance expressions resulting from the cavity model are relatively simple compared to the full-wave model results, the infinite series has to be truncated in practical calculations. The error associated with this truncation depends on the location and the dimensions of the feed port [7].

In order to estimate the power-bus noise level due to a particular source without running a complicated simulation, a closed-form analytical expression for the input and transfer impedance of power-return plane structures is preferred. In particular, a closed-form expression for the upperbound limit of the power-bus input and the transfer impedance can be used to calculate the maximum noise level. Designers could use the expression to check whether signal integrity might be degraded, to evaluate the effects of various geometric and material parameters on the noise level, or to develop general design guidelines for power buses.

Based on solutions of the two-dimensional (2-D) Helmholtz equation in cylindrical coordinates, a closed-form expression for the input impedance of lossless circular parallel plate structures has been developed in [8]. In this paper, the closed-form expression is modified by a complex propagation

Manuscript received August 9, 2002; revised March 17, 2003.

M. Xu is with Hewlett Packard, San Diego, CA 92127-1801 USA.

T. H. Hubing is with the Department of Electrical and Computer Engineering, University of Missouri-Rolla, Rolla, MO 65409 USA (e-mail: hubing@umr.edu).

Digital Object Identifier 10.1109/TEMC.2003.815531

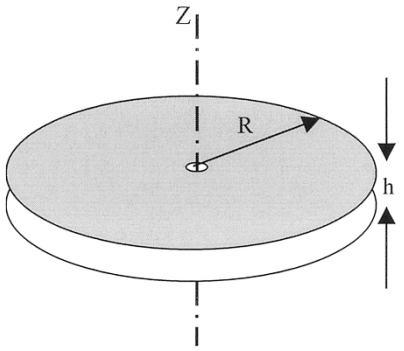

Fig. 1. Geometry of the circular parallel plate structure with a $\boldsymbol{Z}$-directional feed.

constant to include dielectric and conductive losses. A relatively simple analytical expression for the upperbound limit of the input impedance is then derived for general circular power-return plane structures with imperfect conductors and lossy dielectrics. In high-loss power-return plane structures where the board resonances are significantly damped, the input impedance is an upper bound on the transfer impedance between any two points on the board and the exact shape of the boundaries is not critical. Consequently, the closed-form expression for lossy circular parallel plates provides an upper bound on the power-bus transfer impedance between any two ports in high-loss boards of any shape.

II. Modeling Closely-Spaced Circular Power-Return Plane Pairs

The geometry under study is illustrated in Fig. 1. The circular power and return planes have the same radius $\boldsymbol{R}$ and are parallel to each other. A thin layer of dielectric with thickness $\boldsymbol{h}$ separates the planes. The noise current generated by the active devices is modeled as a $\boldsymbol{Z}$-directed current source located at the geometric center of the circular parallel plane pair. The cross section of the coaxial current feed is represented by an electrically small circle of radius $\boldsymbol{r}_0$. When the spacing between the power and the return planes ($\boldsymbol{h}$) is less than a half wavelength at the highest frequency under study, the only modes supported by the structure are the radial transmission-line modes with no variation in the $\boldsymbol{Z}$ and $\boldsymbol{\Phi}$ directions. For a lossless circular power-return plane pair, only the $\boldsymbol{Ez}$ and $\boldsymbol{H_\Phi}$ components are nonzero [8]. Solving the 2-D Helmholtz equation in cylindrical coordinates yields

$$\begin{aligned} E_z &= AH_0^{(1)}(kr) + BH_0^{(2)}(kr) \\ H_\Phi &= \frac{j}{\eta}\left[AH_1^{(1)}(kr) + BH_1^{(2)}(kr)\right] \end{aligned} \tag{2}$$

where A and B are arbitrary constants depending on the source and boundary conditions. In (2), $\boldsymbol{r}$ is the radial distance from the center, and $k = \omega\sqrt{\mu\varepsilon}$ is the real-valued radial wave number for the lossless structure. $H_0^{(1)}(kr)$ and $H_1^{(1)}(kr)$ are the zeroth and the first-order Hankel functions of the first kind representing the inward traveling wave. Similarly, $H_0^{(2)}(kr)$ and $H_1^{(2)}(kr)$ are the zeroth and the first-order Hankel functions of the second kind representing the outward traveling wave.

Since $\boldsymbol{Ez}$ has no variation in the $\boldsymbol{Z}$ direction and $\boldsymbol{H_\Phi}$ has no variation in the $\boldsymbol{\Phi}$ direction, it is possible to uniquely define the $\boldsymbol{Z}$-direction voltage and the radial current as

$$V = -E_z h, \quad I = 2\pi r H_\Phi. \tag{3}$$

With the source condition $I = I_0$ at $\boldsymbol{r}_0$ and the boundary condition $H_\Phi = 0$ at $\boldsymbol{r} = \boldsymbol{R}$ (assuming the structure is bounded by PMC walls), A and B in (2) can be uniquely determined. The input impedance at $\boldsymbol{r}_0$ is then given by the following closed-form expression [8]

$$Z_{\text{in}} = \left.\frac{V}{I}\right|_{r=r_0} = \frac{j\boldsymbol{\eta}h}{2\pi r_0}\frac{J_0(kr_0)N_1(kR) - N_0(kr_0)J_1(kR)}{J_1(kr_0)N_1(kR) - N_1(kr_0)J_1(kR)} \tag{4}$$

where $\boldsymbol{J}_0(\boldsymbol{x})$ and $\boldsymbol{J}_1(\boldsymbol{x})$ are the zeroth and first-order Bessel functions of the first kind, $\boldsymbol{N}_0(\boldsymbol{x})$ and $\boldsymbol{N}_1(\boldsymbol{x})$ are the zeroth and first-order Bessel functions of the second kind.

Power-return plane structures in real products are made of imperfect conductors and imperfect dielectric substrates. For these geometries, the input impedance expression given in (4) need to be modified by replacing the wave number with a complex propagation constant that incorporates the dielectric and conductive losses. If the planes are made of good conductors and the planes are much thicker than a skin depth of the conductor, a complex propagation constant for electrically thin power-return plane structures of arbitrary shape is given by [9]

$$\gamma = j\omega\sqrt{\varepsilon\mu}\sqrt{\left(1 - \frac{j(1+j)\delta_s}{h}\right)(1 - j\tan\delta)} \tag{5}$$

where $\tan\delta$ is the loss tangent of the dielectric substrate. In (5), δ_s is the skin depth of the conductor given by

$$\delta_s = \sqrt{\frac{1}{\pi f \mu \sigma}} \tag{6}$$

where σ is the conductivity of the plane conductor.

The presence of imperfect conductor planes creates a finite tangential electric field, E_T, corresponding to the current flowing along the conductor. However, the magnitudes of the tangential electric field are generally trivial compared to the magnitudes of the normal electric field in most PCB and MCM designs [9]. At the boundary between the power planes and the dielectric substrates, the electric fields are still nearly perpendicular to the planes. Consequently, we can still approximately define the voltage between two planes and the radial current. Using the same source condition $I = I_0$ at $\boldsymbol{r}_0$, and the boundary condition $H_\Phi = 0$ at $r = \boldsymbol{R}$, the input impedance of a lossy circular power-return plane pair evaluated at $\boldsymbol{r}_0$ is given by

$$\begin{aligned} Z_{\text{in}} &= \left.\frac{V}{I}\right|_{r=r_0} \\ &= jZ_o(r_0) \\ &\quad \times \frac{J_0(-j\gamma r_0)N_1(-j\gamma R) - N_0(-j\gamma r_0)J_1(-j\gamma R)}{J_1(-j\gamma r_0)N_1(-j\gamma R) - N_1(-j\gamma r_0)J_1(-j\gamma R)} \end{aligned} \tag{7}$$

where

$$Z_0(r_0) = \frac{h\eta}{2\pi r_0}\sqrt{\frac{\left(1 - \frac{j(1+j)\delta_s}{h}\right)}{(1 - j\tan\delta)}}. \tag{8}$$

The input impedance of a circular power-return plane pair given in (7) is comprised of six Bessel functions with complex arguments. Four out of the six Bessel functions are functions of the feed port radius $\boldsymbol{r}_0$. For power-return plane structures in PCBs and MCMs, the feed port radii are usually electrically small and the structures are generally not over damped. In such case, these four terms related to the feed port radius can be simplified using the small-argument approximations of the Bessel functions resulting in

$$
\begin{aligned}
J_0(-j\gamma r_0) &\approx 1+j\frac{\alpha\beta {r_0}^2}{2}+O\left({r_0}^4\right)\\
N_0(-j\gamma r_0) &\approx \frac{2}{\pi}\left[\mathrm{Eu}+\log\left(\frac{-j\gamma r_0}{2}\right)\right]\\
J_1(-j\gamma r_0) &\approx \frac{-j\gamma r_0}{2}\left(1+j\frac{\alpha\beta {r_0}^2}{8}\right)+O\left({r_0}^5\right)\\
N_1(-j\gamma r_0) &\approx \frac{2}{j\pi\gamma r_0}-\frac{j\alpha r_0}{\pi}\\
&\quad\times\left[\mathrm{Eu}+\log\frac{\beta r_0}{2}-0.5-\frac{1-j\frac{\alpha}{\beta}}{2j\frac{\alpha}{\beta}}\log\left(1-j\frac{\alpha}{\beta}\right)\right]\\
&\text{if}\quad \beta r_0 \ll 1 \quad\text{and}\quad a<\beta. \qquad (9)
\end{aligned}
$$

In (9), α and β are the real and the imaginary part of the propagation constant, γ, respectively. $\mathrm{Eu}\approx 0.5772$ is the Euler constant. A detailed derivation of (9) is provided in the appendix.

Assuming the circular power-return plane structure is electrically large, and the feed port radius is small, it can be shown that the magnitude of the input impedance for a circular power-return plane structure reaches its maximum around $\beta R = n\pi + (\pi/4)(n=1,2,3\ldots)$. An upperbound envelope can be found for the magnitude of the input impedance as

$$
\begin{aligned}
|Z_{\mathrm{in}}| \le |Z_{\mathrm{upper}}| &\approx \frac{\pi h f\mu}{2}\left|1-\frac{j(1+j)\delta_s}{h}\right|\\
&\quad\times\left[\frac{e^{2\alpha R}+1}{e^{2\alpha R}-1}+\frac{2}{\pi}\left|\mathrm{Eu}+\log\left(\frac{-j\gamma r_0}{2}\right)\right|\right]\\
&\text{if}\quad \beta r_0 \ll 1;\quad a<\beta;\quad |\gamma R|\gg 1. \qquad (10)
\end{aligned}
$$

The derivation of (10) is detailed in the appendix.

The upperbound envelope given in (10) is a relatively simple analytical function of the frequency, the dimensions of structures, the dimensions of the feed port, and the spacing between the power and return planes. It is also a function of the material parameters of the circular power-return plane structure. To validate this expression, the input impedance and its upperbound envelope were calculated for two circular boards using (7) and (10), respectively. The radius of each test board was 3.8 cm. Both boards were fed by circular current sources at their geometric centers. The radius of the feed port was 5 mils for both boards. The two circular planes in one test board were separated by a layer of 19.2-mil thick FR4 with a relative permittivity of 3.92 and a loss tangent equal to 0.021. The second board employed a layer of 4.0-mil EmCap[1] material with a relative permittivity of 36 and a loss tangent of 0.015. The calculated input impedances between 1 MHz and 5 GHz are plotted

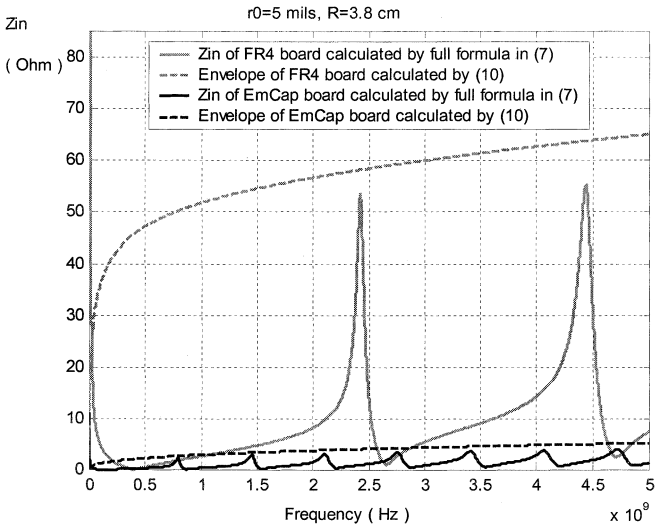

Fig. 2. Input impedances for circular FR4 and EmCap boards.

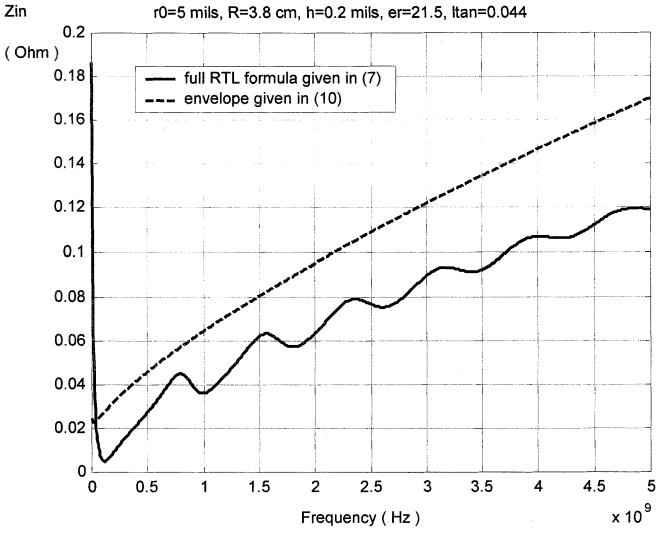

Fig. 3. Input impedance for a circular C-Ply board.

in Fig. 2. The input impedance of the FR4 board has two resonances around 2.425 and 4.438 GHz corresponding to $\beta R \approx (5\pi/4)$ and $\beta R \approx (9\pi/4)$, respectively. Though the upperbound envelope calculated using (10) does not exactly match the peaks at these two resonance frequencies, the difference is within 15%. The EmCap board exhibits more resonances than the FR4 board because of the much higher relative permittivity of the dielectric substrate. But the resonance peaks in the EmCap board are more damped compared to the FR4 board. Around the resonance frequencies, the upperbound envelope predicted by (10) is about 20% higher than the input impedance for the EmCap board.

Fig. 3 plots the calculated input impedance and the upperbound envelope for another circular board. The radius of this power-return plane structure was also equal to 3.8 cm. The dielectric substrate in this board was a layer of 0.2-mil C-Ply[2] material with a relative permittivity of 21.5 and a loss tangent equal to 0.044. The feed port was located at the geometric

[1]EmCap is a registered trademark of Sanmina Corporation.

[2]C-Ply is a registered trademark of 3M Corporation.

center with a radius of 5 mils as in the previous two boards. The input impedance of the C-Ply board was significantly damped as demonstrated in Fig. 3. The envelope predicted by (10) is about 30% higher than the resonance peaks of the calculated input impedance using (7) for this lossy power-return plane structure.

The modeling results suggest that the difference between the upperbound envelope and the input impedance around resonances is more prominent for lossy circular power-return plane structures. To develop a better approximation for high-loss structures, the characteristic impedance of the radial transmission line is used to estimate the input impedance of a circular power-return plane structure.

According to the relation between the Hankel function and the Bessel function of the same order, the $\boldsymbol{Z}$-direction voltage and the radial current can also be expressed in traveling-wave solutions as

$$\begin{aligned} V &= -hG_0(-j\gamma r)\left[Ae^{j\theta(-j\gamma r)} + Be^{-j\theta(-j\gamma r)}\right] \\ &= V^- + V^+ \\ I &= \frac{jhG_1(-j\gamma r)}{Z_0(r)}\left[Ae^{j\phi(-j\gamma r)} + Be^{-j\phi(-j\gamma r)}\right] \\ &= I^- + I^+ \end{aligned} \tag{11}$$

where

$$\begin{aligned} G_0(-j\gamma r) &= \sqrt{{J_0}^2(-j\gamma r) + {N_0}^2(-j\gamma r)} \\ \theta(-j\gamma r) &= \tan^{-1}\left[\frac{N_0(-j\gamma r)}{J_0(-j\gamma r)}\right] \\ G_1(-j\gamma r) &= \sqrt{{J_1}^2(-j\gamma r) + {N_1}^2(-j\gamma r)} \\ \phi(-j\gamma r) &= \tan^{-1}\left[\frac{N_1(-j\gamma r)}{J_1(-j\gamma r)}\right]. \end{aligned} \tag{12}$$

Accordingly, the wave impedance can be calculated as

$$\begin{aligned} Z^- &= \frac{V^-}{I^-} = -Z_c e^{j\left[\theta-\phi+\frac{\pi}{2}\right]} \\ Z^+ &= \frac{V^+}{I^+} = Z_c e^{-j\left[\theta-\phi+\frac{\pi}{2}\right]} \end{aligned} \tag{13}$$

where Z_c is the characteristic impedance of the lossy radial transmission line. According to (11)–(13)

$$Z_c(r) = \frac{Z_0(r)G_0(-j\gamma r)}{G_1(-j\gamma r)}. \tag{14}$$

When $\alpha \geq 0.5\beta$, board resonances are essentially eliminated. The input impedance of such high-loss structures can be accurately approximated by the characteristic impedance evaluated at the feed ports

$$Z_{\text{in}} \approx Z_c(r_0) = \frac{Z_0(r_0)G_0(-j\gamma r_0)}{G_1(-j\gamma r_0)}. \tag{15}$$

If the feed port radius is electrically small at all frequencies of interest, the expression in (15) can be simplified using the small-argument approximations given in (9). In particular, when

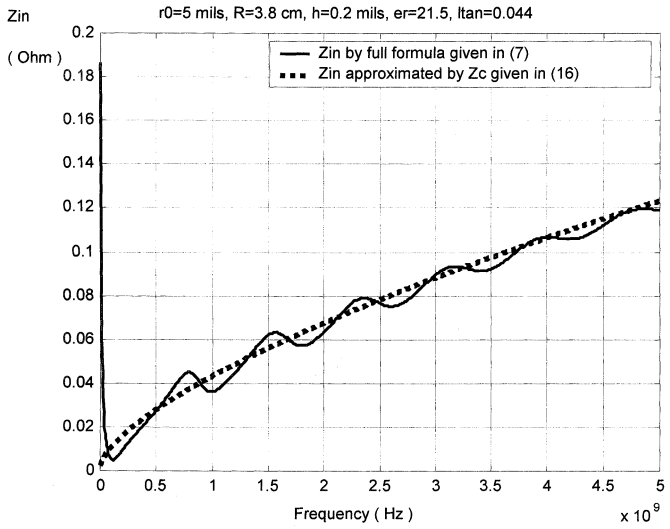

Fig. 4. Input impedance and the characteristic impedance of a circular C-Ply board.

$\beta r_0 \ll 1$ such that and $|J_0(-j\gamma r_0)| \ll |N_0(-j\gamma r_0)|$ and $|J_1(-j\gamma r_0)| \ll |N_1(-j\gamma r_0)|$, (15) can be further reduced to

$$|Z_{\text{in}}| \approx |Z_c(r_0)| \approx \left| f\mu(1+j)\delta_s \left[\text{Eu} + \log\left(\frac{-j\gamma r_0}{2}\right)\right]\right|. \tag{16}$$

Fig. 4 plots the input impedance of the 0.2-mil C-Ply board and its approximation using the characteristic impedance given in (16). Compared to the envelope given in (10), the characteristic impedance is a better approximation to the input impedance for this high-loss board.

In summary, the expressions given in (5), (10), and (16) can be used to estimate the input impedance of a center-fed circular power-return plane structure without running numerical simulations. First, the complex propagation constant of the structure, γ, can be calculated according to (5) using the geometrical and material parameters. For low loss structures, where the real part of γ is much less than the imaginary part of γ, an upperbound envelope of the input impedance can be calculated using (10). For high-loss structures where the real part of γ is approaching or greater than one-half of the imaginary part of γ, the input impedance can be approximated using the characteristic impedance given in (16).

III. High-Loss Power-Return Plane Structures of Arbitrary Shape

The expression given in (10) predicts an upperbound envelope for the magnitude of the input impedance of a circular power-return plane structure assuming the structure is fed at its geometric center. However, power-return plane structures in PCBs and MCMs are generally not circular and the feed and observation ports are not necessarily at the geometric centers of the structures. As a result, the magnitudes of the power-bus input and transfer impedance are not only determined by the board dimensions, the port dimensions, the spacing between the planes, and the loss in the structure, but they are also affected by the shape of the structure and the relative port locations on the board.

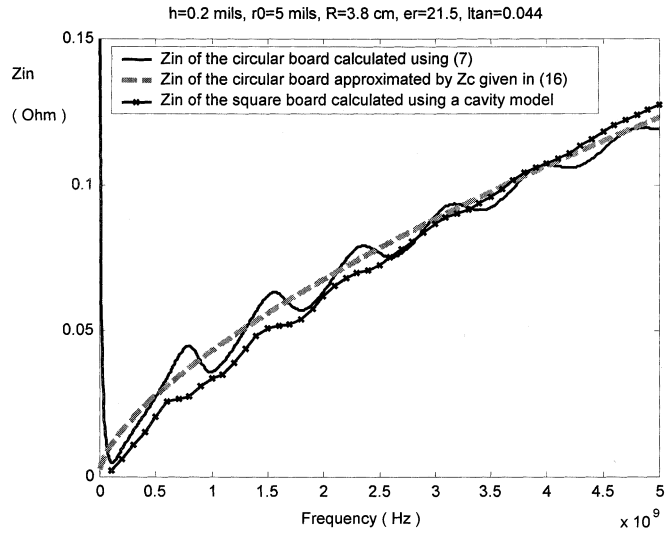

Fig. 5. Input impedance of circular and square C-Ply boards.

However, for high-loss power-return plane structures where the board resonances are significantly damped or essentially eliminated, the exact shape of the board edges does not have a significant effect on the power-bus impedance. The maximum amplitude of a wave reflected from a board edge is proportional to $e^{-2\alpha D}$, where D is the shortest distance from the feeding point to the board edge. When the value of this factor is below a given threshold (e.g., 5%), the impact that the exact shape of the board has on the feed point impedance may no longer be considered to be significant.

Embedded capacitance boards are good examples of PCBs with high-loss power-return plane structures [10]. For such high-loss structures, as long as the ports are not near the edges, the simplified expressions developed for the circular structures can be used to estimate the input impedance of an arbitrarily shaped board. Fig. 5 compares the calculated input impedance of a 7.6 by 7.6-cm square board to the input impedance of a circular board with a diameter equal to 7.6 cm. Both boards are fed at the geometric center with a $\boldsymbol{Z}$-directed current probe. The feed wire radius is 5-mils for both boards. The power and the return planes in both structures are separated by a layer of 0.2-mil C-Ply material. The input impedance of the square board is calculated using the cavity model [9]. The input impedance of the circular board is calculated using the full formula in (7) and approximated by the characteristic impedance at the feed port using (16). As we can see, the power-bus resonance frequencies are determined by the edges. However, since the power-bus resonances are significantly damped in these C-Ply boards, the approximate calculation in (16) can be used to provide a good estimate of the power-bus impedance for the square board.

IV. Conclusion

A closed-form estimate for the input impedance of circular power-return plane structures has been developed. The dielectric and conductive losses are incorporated in a complex propagation constant. When the feed port is small compared to a wavelength and the structure is not over-damped, the upper-bound envelope of the input impedance can be calculated using a simple analytical expression based on geometric and material parameters. For high-loss structures, a better approximation for the input impedance is the characteristic impedance of the circular power-return plane structure. Since the board resonances are significantly damped in high-loss power return plane structures, the exact shape of the board does not have a significant effect on the input impedance. Consequently, the closed-form expression developed for circular structures can be used to estimate the input impedance of power-return plane pairs of any shape.

Appendix
Evaluation of the Upperbound Envelope for the Input Impedance of a Circular Power-Return Plane Structure

With conductive and dielectric losses, the input impedance of a center-fed circular power-return plane structure is given by

$$Z_{\text{in}} = jZ_o(r_0) \times \frac{J_0(-j\gamma r_0)N_1(-j\gamma R) - N_0(-j\gamma r_0)J_1(-j\gamma R)}{J_1(-j\gamma r_0)N_1(-j\gamma R) - N_1(-j\gamma r_0)J_1(-j\gamma R)} \tag{A1}$$

where

$$\gamma = \alpha + j\beta = j\omega\sqrt{\varepsilon\mu}\sqrt{\left(1 - \frac{j(1+j)\delta_s}{h}\right)(1 - j\tan\delta)} \tag{A2}$$

and

$$Z_0(r_0) = \frac{h\eta}{2\pi r_0}\sqrt{\frac{\left(1 - \frac{j(1+j)\delta_s}{h}\right)}{(1 - j\tan\delta)}}. \tag{A3}$$

This expression contains six Bessel functions with complex arguments. Four out of the six Bessel functions are dependent on the feed port radius $\boldsymbol{r_0}$. If the feed port radius is electrically small and the structure is not over damped, these four terms related to the feed port radius can be simplified using small-argument approximations of the Bessel functions.

A. Small-Argument Approximation of $J_0(-j\gamma r_0)$

According to the addition theorems [11], for Bessel functions of the first kind with general arguments u and v, if $|v| < |u|$

$$J_m(u \pm v) = \sum_{r=-\infty}^{\infty} J_r(v)J_{m\mp r}(u). \tag{A4}$$

In (A4), the orders $\boldsymbol{r}$ and $\boldsymbol{m}$ of the Bessel functions are arbitrary integers. Furthermore, for Bessel functions of integer order $\boldsymbol{n}$, according to [11], [12]

$$J_{-n}(z) = (-1)^n J_n(z) = J_n(-z)$$
$$N_{-n}(z) = (-1)^n N_n(z). \tag{A5}$$

And the Bessel functions with pure imaginary arguments are related to the modified Bessel functions as [11], [12]

$$I_n(z) = j^{-n} J_n(jz) = \sum_{m=0}^{\infty} \frac{(0.5x)^{n+2m}}{m!\Gamma(n+m+1)}. \tag{A6}$$

Using (A4)–(A6), the term $J_0(-j\gamma r_0)$ can be expanded into

$$\begin{aligned} J_0(-j\gamma r_0) &= J_0(\beta r_0 - j\alpha r_0) \\ &= 2\sum_{m=1}^{\infty} J_m(\beta r_0) I_m(\alpha r_0) j^m \\ &\quad + J_0(\beta r_0) I_0(\alpha r_0). \end{aligned} \tag{A7}$$

The Bessel functions with small arguments can be approximated as [13]

$$\begin{aligned} J_0(x) &\approx 1 \\ N_0(x) &\approx \frac{2}{\pi}\left[\mathrm{Eu} + \log\frac{x}{2}\right] \\ J_n(x) &\approx \frac{1}{n!}\left(\frac{x}{2}\right)^n \\ N_n(x) &\approx -\frac{(n-1)!}{\pi}\left(\frac{2}{x}\right)^n, \qquad \text{for } n > 0. \end{aligned}$$

In (A8), $\mathrm{Eu} \approx 0.5772$ is the Euler constant. Using (A8), when the feed wire radius $\boldsymbol{r}_0$ is very small compared to a wavelength, $J_0(-j\gamma r_0)$ can be approximated by

$$J_0(-j\gamma r_0) \approx 1 + j\frac{\alpha\beta {r_0}^2}{2} + O\left(r_0^4\right). \tag{A9}$$

B. Small-Argument Approximation of $N_0(-j\gamma r_0)$

Similar to (A4), for Bessel functions of the second kind with general arguments u and v, if $|v| < |u|$

$$N_m(u \pm v) = \sum_{r=-\infty}^{\infty} J_r(v) N_{m\mp r}(u). \tag{A10}$$

In (A10), the orders $\boldsymbol{r}$ and $\boldsymbol{m}$ of the Bessel functions are arbitrary integers [11]. If $\alpha < \beta$, the term $N_0(-j\gamma r_0)$ can be expanded to

$$N_0(-j\gamma r_0) = 2\sum_{m=1}^{\infty} N_m(\beta r_0) I_m(\alpha r_0) j^m + N_0(\beta r_0) I_0(\alpha r_0). \tag{A11}$$

When the feed-wire radius $\boldsymbol{r}_0$ is very small compared with a wavelength, using the small-argument approximations given in (A8), $N_0(-j\gamma r_0)$ can be approximated by

$$N_0(-j\gamma r_0) \approx \frac{2}{\pi}\left[\mathrm{Eu} + \log\frac{\beta r_0}{2}\right] - \frac{2}{\pi}\sum_{m=1}^{\infty} \frac{\left(j\frac{\alpha}{\beta}\right)^m}{m}. \tag{A12}$$

When $\alpha < \beta$, (A12) can be simplified using binomial expansions resulting in

$$\begin{aligned} N_0(-j\gamma r_0) &\approx \frac{2}{\pi}\left[\mathrm{Eu} + \log\frac{\beta r_0}{2} + \log\left(1 - j\frac{\alpha}{\beta}\right)\right] \\ &= \frac{2}{\pi}\left[\mathrm{Eu} + \log\left(\frac{-j\gamma r_0}{2}\right)\right]. \end{aligned} \tag{A13}$$

C. Small-Argument Approximation of $J_1(-j\gamma r_0)$

According to (A4)–(A6), when $\alpha < \beta$, $J_1(-j\gamma r_0)$ can be expanded to

$$\begin{aligned} J_1(-j\gamma r_0) = J_1(\beta r_0) I_0(\alpha r_0) &+ \sum_{m=1}^{\infty} J_{m+1}(\beta r_0) I_m(\alpha r_0) j^m \\ &- \sum_{m=1}^{\infty} J_{m-1}(\beta r_0) I_m(\alpha r_0) j^m. \end{aligned} \tag{A14}$$

When the feed-wire radius $\boldsymbol{r}_0$ is very small compared to a wavelength, using the small-argument approximations given in (A8) yields

$$J_1(-j\gamma r_0) \approx \frac{-j\gamma r_0}{2}\left(1 + j\frac{\alpha\beta {r_0}^2}{8}\right) + O\left({r_0}^5\right). \tag{A15}$$

D. The Small-Argument Approximation of $N_1(-j\gamma r_0)$

According to (A4)–(A6), when $\alpha < \beta$, $N_1(-j\gamma r_0)$ can be expanded to

$$\begin{aligned} N_1(-j\gamma r_0) = &-jN_0(\beta r_0) I_1(\alpha r_0) + N_1(\beta r_0) I_0(\alpha r_0) \\ &+ \sum_{m=1}^{\infty} N_{m+1}(\beta r_0) I_m(\alpha r_0) j^m \\ &- \sum_{m=2}^{\infty} N_{m-1}(\beta r_0) I_m(\alpha r_0) j^m. \end{aligned} \tag{A16}$$

When the feed-wire radius $\boldsymbol{r}_0$ is very small compared to a wavelength, the first two terms in (A16) can be simplified using the small-argument approximations given in (A8) as

$$\begin{aligned} &-jN_0(\beta r_0) I_1(\alpha r_0) + N_1(\beta r_0) I_0(\alpha r_0) \\ &\approx \frac{-j\alpha r_0}{\pi}\left[\mathrm{Eu} + \log\frac{\beta r_0}{2}\right] - \frac{2}{\pi\beta r_0} \end{aligned} \tag{A17}$$

Using the small-argument approximations on the two series terms in (A16) yields

$$\begin{aligned} &\sum_{m=1}^{\infty} N_{m+1}(\beta r_0) I_m(\alpha r_0) j^m - \sum_{m=2}^{\infty} N_{m-1}(\beta r_0) I_m(\alpha r_0) j^m \\ &\quad \approx -\frac{2}{\pi\beta r_0}\sum_{m=1}^{\infty}\left(\frac{j\alpha}{\beta}\right)^m + \frac{j\alpha r_0}{2\pi}\sum_{m=1}^{\infty}\frac{1}{m(m+1)}\left(\frac{j\alpha}{\beta}\right)^m. \end{aligned} \tag{A18}$$

Since $\alpha < \beta$, expression in (A18) can be approximated by

$$\sum_{m=1}^{\infty} N_{m+1}(\beta r_0) I_m(\alpha r_0) j^m - \sum_{m=2}^{\infty} N_{m-1}(\beta r_0) I_m(\alpha r_0) j^m \approx -\frac{2}{\pi\beta r_0} \frac{j\frac{\alpha}{\beta}}{1 - j\frac{\alpha}{\beta}} + \frac{j\alpha r_0}{2\pi} \left[1 + \frac{1 - j\frac{\alpha}{\beta}}{j\frac{\alpha}{\beta}} \log\left(1 - j\frac{\alpha}{\beta}\right)\right]. \quad \text{(A19)}$$

Substituting (A17) and (A19) into (A16) yields

$$N_1(-j\gamma r_0) \approx \frac{2}{j\pi\gamma r_0} - \frac{j\alpha r_0}{\pi} \times \left[\mathrm{Eu} + \log\frac{\beta r_0}{2} - 0.5 - \frac{1 - j\frac{\alpha}{\beta}}{2j\frac{\alpha}{\beta}} \log\left(1 - j\frac{\alpha}{\beta}\right)\right] \approx \frac{2}{j\pi\gamma r_0} \quad \text{(A20)}$$

E. Upperbound Envelope for the Input Impedance of the Circular Power-Return Plane Structure With Center Feeding

According to the small-argument approximations of $J_0(-j\gamma r_0)$, $N_0(-j\gamma r_0)$, $J_1(-j\gamma r_0)$, and $N_1(-j\gamma r_0)$ given in (A9), (A13), (A15) and (A20) respectively, if $\boldsymbol{r}_0$ approaches to 0

$$|J_0(-j\gamma r_0)| \to 1 \quad |J_1(-j\gamma r_0)| \to 0$$
$$|N_0(-j\gamma r_0)| \to \infty \quad |N_1(-j\gamma r_0)| \to \infty. \quad \text{(A21)}$$

In addition, for electrically large circular power-return plane structures where $|\gamma R| \gg 0$, the magnitude of $N_1(-j\gamma R)$ and the magnitude of $J_1(-j\gamma R)$ are of the same order. As a result

$$|J_1(-j\gamma r_0) N_1(-j\gamma R)| \ll |N_1(-j\gamma r_0) J_1(-j\gamma R)|. \quad \text{(A22)}$$

Consequently, for an electrically large circular power-return plane structure with an electrically small feed port, the magnitude of the input impedance in (A1) can be approximated by

$$|Z_{\mathrm{in}}| \approx \frac{|Z_o(r_0)|}{|N_1(-j\gamma r_0)|} \left|\frac{N_1(-j\gamma R)}{J_1(-j\gamma R)} - N_0(-j\gamma r_0)\right|. \quad \text{(A23)}$$

Applying the Minkowski inequality to (A23) yields an upper bound limit for the input impedance

$$|Z_{\mathrm{in}}| \le |Z_{\mathrm{upper}}| = \frac{|Z_o(r_0)|}{|N_1(-j\gamma r_0)|} \left[\left|\frac{N_1(-j\gamma R)}{J_1(-j\gamma R)}\right| + |N_0(-j\gamma r_0)|\right]. \quad \text{(A24)}$$

In (A24), $|Z_o(r_0)|/|N_1(-j\gamma r_0)|$ and $|N_0(-j\gamma r_0)|$ are monotonic in the vicinity of $\boldsymbol{r}_0 = 0$. $|(N_1(-j\gamma R))/(J_1(-j\gamma R))|$ is the only term in the expression that oscillates. Therefore, $|Z_{\mathrm{upper}}|$ peaks when $|(N_1(-j\gamma R))/(J_1(-j\gamma R))|$ reaches its maximums. When the board is electrically large, large-argument approximations of the Bessel functions can be applied [13]

$$J_1(-j\gamma R) = \sqrt{\frac{2}{\pi x}} \frac{e^{(\gamma R - j\frac{3\pi}{4})} + e^{-(\gamma R - j\frac{3\pi}{4})}}{2}$$
$$N_1(-j\gamma R) = \sqrt{\frac{2}{\pi x}} \frac{e^{(\gamma R - j\frac{3\pi}{4})} - e^{-(\gamma R - j\frac{3\pi}{4})}}{2j}. \quad \text{(A25)}$$

$|(N_1(-j\gamma R))/(J_1(-j\gamma R))|$ reaches its peaks when $\beta R = n\pi + (\pi/4)$ (where $n = 1, 2, 3\ldots$). And the maximum of $|(N_1(-j\gamma R))/(J_1(-j\gamma R))|$ is given by

$$\left|\frac{N_1(-j\gamma R)}{J_1(-j\gamma R)}\right|_{\max} = \frac{e^{2\alpha R} + 1}{e^{2\alpha R} - 1}. \quad \text{(A26)}$$

Consequently

$$|Z_{\mathrm{in}}| \le |Z_{\mathrm{upper}}|_{\max} = \left|\frac{jZ_o(r_0)}{-N_1(-j\gamma r_0)}\right| \times \left[\frac{e^{2\alpha R} + 1}{e^{2\alpha R} - 1} + |N_0(-j\gamma r_0)|\right]. \quad \text{(A27)}$$

This expression can be further simplified using the approximations given in (A13) and (A20)

$$|Z_{\mathrm{in}}| \le |Z_{\mathrm{upper}}| \approx \left|\frac{\pi\gamma r_0 Z_o(r_0)}{2}\right| \times \left[\frac{e^{2\alpha R} + 1}{e^{2\alpha R} - 1} + \frac{\pi}{2}\left|\mathrm{Eu} + \log\left(\frac{-j\gamma r_0}{2}\right)\right|\right]. \quad \text{(A28)}$$

Equation (A28) can be used to determine an upper bound for the input impedance of a general circular power-return plane structure assuming the structure is electrically large and the feed port (located at the geometric center of the structure) is electrically small.

REFERENCES

[1] T. P. Van Doren, "Power bus noise estimation algorithm," UMR Electromagnetic Compatibility Laboratory, Univ. Missouri, Rolla, MO, TR99-3-024, Mar. 1999.

[2] L. Smith, R. Anderson, D. Forehand, T. Pelc, and T. Roy, "Power distribution system design methodology and capacitor selection for modern CMOS technology," *IEEE Trans. Adv. Packag.*, vol. 22, pp. 284–291, Aug. 1999.

[3] H. Johnson and M. Graham, *High-Speed Digital Design: A Handbook of Black Magic*. Englewood Cliffs, NJ: Prentice-Hall, 1993, ch. 8.

[4] G. T. Lei, R. W.Robert W. Techentin, and B. K.Barry K. Gilbert, "High-frequency characterization of power/ground-plane structures," *IEEE Trans. Microwave Theory Tech.*, vol. 47, pp. 562–569, May 1999.

[5] T. Okoshi, *Planar Circuits for Microwaves and Lightwaves*. New York: Springer-Verlag, 1985, ch. 2.

[6] Z. L. Wang, O. Wada, Y. Toyota, and R. Koga, "An improved closed-form expression for accurate and rapid calculation of power/ground plane impedance in multilayer PCBs," in *Proc. Symp. Electromagnetic Theory*, Toyama, Japan, Oct. 2000, EMT-00-68.

[7] M. Xu, Y. Ji, T. H. Hubing, T. Van Doren, and J. Drewniak, "Development of a closed-form expression for the input impedance of power-ground plane structures," in *Proc. IEEE Int. Symp. Electromagnetic Compatibility*, Washington, DC, Aug. 2000, pp. 77–82.

[8] S. Ramo and J. R.J. R. Whinnery, *Fields and Waves in Modern Radio*, 2nd ed. New York: Wiley, 1953, ch. 8.

[9] M. Xu, H. Wang, and T. H. Hubing, "Application of the cavity model to lossy power-return plane structure in printed circuit boards," *IEEE Trans. Adv. Packag.*, vol. 26, pp. 73–80, Feb. 2003.

[10] M. Xu, T. H. Hubing, J. Chen, T. P. Van Doren, J. L. Drewniak, and R. E. DuBroff, "Power-bus decoupling with embedded capacitance in printed circuit board design," *IEEE Trans. Electromagn. Compat.*, vol. 45, pp. 22–30, Feb. 2003.
[11] N. W. McLachlan, *Bessel Functions for Engineers*. London, U.K.: Oxford Univ.Press, 1961, pp. 190–206.
[12] G. N. Watson, *A Treatise on the Theory of Bessel Functions*. New York: Cambridge Univ. Press, 1958, ch. 5 and 7.
[13] C. A. Balanis, *Advanced Engineering Electromagnetics*. New York: Wiley, 1989, pp. 934–938.

Minjia Xu (S'98–M'02) was born in Chongquing, China in 1972. She received the B.S. (with honors) and M.S. degrees in electrical engineering from Tsinghua University, Beijing, China, in 1994 and 1997, respectively, and the Ph.D. degree in electrical engineering from the University of Missouri-Rolla in 2001.

From 1998 to 2001, she was with the Electromagnetic Compatibility (EMC) Laboratory, University of Missouri-Rolla. She then joined the Hewlett-Packard Company, San Diego, CA, as an EMC engineer in the All-in-One Personal Printing Division. Her current research interests include numerical and experimental analysis of signal integrity and electromagnetic compatibility issues related to printing and faxing products, development of printed circuit board and system level technology for noise and radiated emission mitigation, as well as design for immunity and electrostatic disturbance conformity.

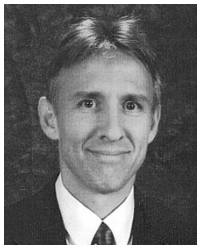

Todd Hubing (S'82–M'82–SM'93) received the B.S.E.E. degree from the Massachusetts Institute of Technology, Cambridge, in 1980, the M.S.E.E. degree from Purdue University, West Lafayette, IN, in 1982, and the Ph.D. degree in electrical engineering from North Carolina State University, Raleigh, in 1988.

He is currently a Professor of Electrical Engineering with the University of Missouri-Rolla (UMR), where he is also a member of the principal faculty in the Electromagnetic Compatibility Laboratory. Prior to joining UMR in 1989, he was an Electromagnetic Compatibility Engineer with IBM, Research Triangle Park, NC. Since joining UMR, the focus of his research has been measuring and modeling sources of electromagnetic interference. He has authored or presented over 100 technical papers, presentations, and reports on electromagnetic modeling and electromagnetic compatibility related subjects.

Dr. Hubing has been a member of the Board of Directors of the IEEE EMC Society since 1995 and is the 2002–2003 President of the Society.